Translational Oncology
www.transonc.com

Volume 12 Number 1 January 2019 pp. 143–153 143

Preclinical *In Vitro* and *In Vivo* Evidence of an Antitumor Effect of CX-4945, a Casein Kinase II Inhibitor, in Cholangiocarcinoma[1,2,3]

Kais Zakharia[*,†,‡,4], Katsuyuki Miyabe[‡,4], Yu Wang[§4], Dehai Wu[‡,4], Catherine D. Moser[‡], Mitesh J. Borad[#] and Lewis R. Roberts[‡]

[*]Internal Medicine Residency Program, Department of Medical Education, Beaumont Health - Dearborn, Oakwood Campus, Dearborn, MI, USA; [†]Division of Gastroenterology and Hepatology, University of Iowa, Iowa City, IA, USA; [‡]Division of Gastroenterology and Hepatology, Mayo Clinic, Rochester, MN, USA; [§]Department of Hepatobiliary Surgery, Nanfang Hospital, Southern Medical University, Guangzhou, China; [#]Division of Hematology, Division of Oncology, Mayo Clinic, Scottsdale, AZ, USA

Abstract

PURPOSE: We investigated the antitumor effect of the casein kinase II (CK2) inhibitor CX-4945 on cholangiocarcinoma (CCA). *METHODS:* We assessed the effect of CX-4945 alone and/or in combination with gemcitabine and cisplatin on cell viability, colony formation, and apoptosis of CCA cell lines and on *in vivo* growth of HuCCT1 xenografts. *RESULTS:* CX-4945 dose-dependently decreased viability of HuCCT1, EGI-1, and Liv27 and decreased phospho-AKT/total AKT and phospho-PTEN/total PTEN ratios. CX-4945 significantly increased caspase 3/7 activity in a dose- and time-dependent manner. CX-4945 significantly enhanced the effect of gemcitabine or cisplatin on HuCCT1, EGI-1, and Liv27 cells and inhibited the phosphorylation of DNA repairing enzymes XRCC1 and MDC1. Further, CX-4945 alone significantly inhibited growth of HuCCT1 mouse xenograft tumors. Combining CX-4945 with gemcitabine and cisplatin was more potent than CX-4945 alone or gemcitabine/cisplatin. The effect of CX-4945 on cell proliferation, apoptosis, the PI3K/AKT pathway, and DNA repair was confirmed in the mouse xenografts. *CONCLUSION:* CX-4945 has an antiproliferative effect on CCA and enhances the effect of gemcitabine and cisplatin through its inhibitory effect on the PI3K/AKT pathway and DNA repair.

Translational Oncology (2019) 12, 143–153

Introduction

Cholangiocarcinoma (CCA) is a highly lethal cancer that arises from the biliary tract epithelium either within the liver (intrahepatic), at the liver hilum (perihilar), or within the distal extrahepatic bile ducts (distal). Worldwide, CCA is the second most common primary liver malignancy after hepatocellular carcinoma. The incidence of intrahepatic CCA increased from 0.07 case per 100,000 in 1973 to 0.73 case per 100,000 in 2010 [1]. Most CCA patients are diagnosed at late stages and are not eligible for the only potentially curative therapies, resection and transplantation. In addition, the standard chemotherapy regimen of gemcitabine and cisplatin is suboptimal in prolonging survival of CCA patients. Thus, there is an urgent need to develop novel more effective therapies against CCA.

Casein kinase II (CK2) is a serine/threonine-selective protein kinase that is a tetramer of two alpha and two beta subunits. CK2 is

Address all correspondence to: Lewis R. Roberts, MB ChB, PhD, Division of Gastroenterology and Hepatology, Mayo Clinic College of Medicine and Science, 200 First Street SW, Rochester, MN 55905.
E-mail: roberts.lewis@mayo.edu

[1] Financial support: This work was supported by National Institutes of Health grant CA165076 (to L. R. R.); the Mayo Clinic Center for Cell Signaling in Gastroenterology (NIDDK P30DK084567); The Cholangiocarcinoma Foundation; the Mayo Clinic Cancer Center (CA15083); and the Mayo Foundation. Its contents are solely the responsibility of the authors and do not necessarily represent the official views of the NIH.
[2] Conflicts of interest: The authors declare no potential conflicts of interest.
[3] Disclosures: none.
[4] These authors contributed equally to this work.

Received 2 September 2018; Revised 8 September 2018; Accepted 8 September 2018

1936-5233/19
https://doi.org/10.1016/j.tranon.2018.09.005

important in different cellular processes, including cell proliferation, cell apoptosis, DNA repair, and cell cycle control [2]. Increased CK2 activity has been implicated in neoplastic transformation and aggressive cell proliferation [3,4]. High CK2 expression has been detected in 66% of CCA tissues and was associated with higher TNM stage, histological grade, and poorer overall survival [5]. CK2 has also been detected in the plasma of patients with CCA and can potentially be used as a biomarker for diagnosis [6]. CX-4945 is a potent and highly selective inhibitor of CK2 [7]. CX-4945 has shown antitumor activity against other human solid cancer cells such as breast cancer [4], pancreatic adenocarcinoma [4], and ovarian carcinoma [8].

The phosphatidylinositol 3-kinase (PI3K)/AKT pathway is a key pathway in multiple vital cellular processes of various cancers including CCA [9,10]. Previous studies on other cancer cell types have shown that CX-4945 has antiproliferative effects through inhibiting the PI3K/AKT pathway, specifically reducing CK2-mediated AKT [4,11,12] and phosphatase and tensin homolog (PTEN) phosphorylation [12,13]. Phosphorylation of PTEN results in its stability from proteasomal degradation and leads to accumulation and functional inactivation of PTEN; therefore, inhibition of PTEN phosphorylation unmasks its tumor suppressor effects.

XRCC1 and MDC1 are DNA repair enzymes that play essential roles in single-strand break (SSB) and double-strand break (DSB) repair, respectively [4]. CK2 has been shown to be a key contributor to the DNA repair response mediated through XRCC1 and MDC1 in ovarian cancer cell lines [4].

In the present study, we hypothesized that CX-4945 exerts an antineoplastic effect on CCA by inhibiting the PI3K/AKT pathway and investigated whether CX-4945 has synergistic or additive effects when combined with standard gemcitabine/cisplatin chemotherapy and whether this effect is mediated through inhibiting the DNA repair response activated by the DNA-damaging agents gemcitabine and cisplatin. Finally, we explored the effects of CX-4945 in the HuCCT1 xenograft model.

Materials and Methods

Reagents

Crystal violet and β-actin antibody were obtained from Sigma. Gemcitabine and cisplatin were purchased from Mayo Pharmacy. Antibodies against P-AKT (S437) (#4060), AKT (#9272), and P-PTEN (#9551) were purchased from Cell Signaling. Antibodies against P-AKT (S129) (#ab133458) and PTEN (#ab32199) were purchased from AbCam. Antibodies against CK2 (#2656) and phospho-CK2 (#8738) were purchased from Cell Signaling. Cell Counting Kit-8 (CCK-8) was purchased from Dojindo Laboratories (Rockville, MD). CX-4945 was a gift from Senhwa Biosciences.

Cell Culture

The HuCCT1 and EGI-1 cell lines were obtained from the Japanese Collection of Research Bioresources and the German Collection of Microorganisms and Cell Cultures, respectively. Liv27 is a novel patient-derived intrahepatic CCA cell line established in our laboratory. HuCCT1 and EGI-1 were cultured in RPMI 1640 with 10% FBS and 1% penicillin-streptomycin. Liv27 was cultured in DMEM/F12 media supplemented with 5% platelet lysate, 0.2% heparin, 1 μg/ml insulin, 0.393 μg/ml dexamethasone, and 1% penicillin-streptomycin. All cells were maintained at 37°C in the presence of 5% CO_2.

Cell Viability Assay

HuCCT1, EGI-1, and Liv27 cells were plated in quadruplicate in 96-well plates at a density of 2000, 4000, and 4000 cells per well, respectively according to the growth characteristics of each cell line. After 24 hours, the cells were treated with CX-4945 for 24, 48, and/or 72 hours. For the combination experiments, cells were incubated for 24 hours and treated with CX-4945 (0, 2.5, 5, 7.5, 10, 15, 20 μM) and gemcitabine (0, 10, 25, 50, 75, 100 nM) or cisplatin (0, 1, 2.5, 5, 7.5, 10 μM) for 72 hours. Cell viability after treatment was assessed using CCK-8 assays. The combination index (CI) was calculated using the Chou Talalay technique to determine whether CX-4945 has synergistic or additive effects when combined with gemcitabine or cisplatin.

Colony Formation Assay

Cells were plated at 500 cells per well in a 6-well plate. After 24 hours, CX-4945 was added, and cells were incubated for 10 days. Cells were then fixed with methanol-acetic acid (3:1) solution and stained with 0.5% crystal violet. The number of colonies, defined as ≥50 cells/colony, was counted manually by light microscopy.

Caspase 3/7 Assay

HuCCT1, EGI-1, and Liv27 cells were plated in quadruplicate in 96-well plates. After 24-hour incubation, the cells were treated with CX-4945 for 24, 48, and 72 hours, then Caspase 3/7 assay reagent was added to each well (ratio of 1:4), and immunofluorescence was measured (excitation and emission wavelengths of 485 and 530 nm, respectively).

ShRNA Mediated Knockdown of DNA Repairing Enzymes. To produce the XRCC1 and MDC1 knockdown CCA cells, we used a pLKO.1 lentiviral vector containing a short hairpin RNA (shRNA). The XRCC1 and MDC1 shRNA constructs were obtained from Sigma Aldrich (MISSION TRC shRNA and targeted the 5′ coding region of the human XRCC1 and MDC1 messenger RNAs). To produce XRCC1- or MDC1-depleted CCA cells, five XRCC1 and MDC1 shRNA constructs were tested, and the construct providing the most robust knockdown was used (MISSION TRC shRNA TRCN0000007913 for XRCC1 and TRCN0000018853 for MDC1). The shRNA constructs have the following hairpin sequences:

XRCC1, CCGGCCAGTGCTCCAGGAAGATATACTCGAG TATATCTTCCTGGAGCACTGGTTTTT;
MDC1, CCGGCCTTCTATCAAGCCAACCGTTCTCGA GAACGGTTGGCTTGATAGAAGGTTTTT.

The nontarget shRNA control plasmid DNA is provided as 10 μg of plasmid DNA in Tris-EDTA buffer at a concentration of 500 ng/μl. ShRNA-expressing retroviruses were produced by cotransfection of the retroviral plasmids psPAX2 and pMD2 at a ratio of 4:3:1 retrospectively. HuCCT1 and EGI-1 cells were infected with shRNA viral supernatant along with 8 μg/ml polybrene (American Bioanalytical, Natick, MA) for 24 hours followed by a 72-hour selection with 1 μg/ml puromycin (Mediatech) to eliminate uninfected cells. We were unable to successfully establish XRCC1 or MDC1 knockdown Liv27 cells because they were not viable.

Western Immunoblotting

Western immunoblotting was used to assess the effects of CX-4945 on the PI3K/AKT pathway and DNA repair enzymes in CCA cells and xenograft tissues. Protein lysates were prepared using the Phospho-Safe cell extraction buffer (Novagen, Germany) according to the

manufacturer's protocol. Equivalent amounts of protein were separated on a 4%-15% Tris-HCl gel and transferred to PVDF membranes. Membranes were blocked with 5% BSA and incubated overnight with primary antibody against P-AKT (S129) (1:1000), P-AKT (S473) (1:2000), AKT (1:1000), P-PTEN (1:1000), PTEN (1:500), P-mTOR (1:1000), mTOR (1:1000), P-p70 S6K (1:1000), p70 S6K (1:1000), P-CK2 (1:1000), CK2 (1:1000), P-MDC1 (1:250), MDC1 (1:250), P-XRCC1 (S485/T488) (1:1000), P-XRCC1 (S518/T519/T523) (1:1000), XRCC1 (1:1000), or β-actin (1:5000). Blots were then incubated with secondary antibodies conjugated with horseradish peroxidase, and signals were visualized using the HyGLO HRP detection kit. β-Actin was measured as the loading control. Quantitation of the signal was performed using ImageJ software.

In Vivo Efficacy Studies

Six- to 8-week-old female athymic nude mice were used. Animals were maintained under clean room conditions in sterile filter top cages. Animals received sterile rodent chow and water *ad libitum*. All animal protocols were approved by the Institutional Animal Care and Use Committee at the Mayo Clinic (#A17215-15). We selected the HuCCT1 CCA cell line for this study because CK2 was highly expressed in this cell line [14]. Xenografts were initiated by subcutaneous injection of HuCCT1 cells with 2 × 106 cells per 200 μl Matrigel (injection volume 200 μl) into the right flank area of each mouse. Tumor volume and body weight were recorded every 3 days. Tumor volume was calculated using the equation: volume = $L \times S2/2$ (L and S represent the longest and the shortest diameter of the tumor, respectively). When tumors reached a volume of 100-200 mm^3, the mice were randomized into 4 groups of 15 mice: 1) group 1: control; 2) group 2: treated with gemcitabine and cisplatin; 3) group 3: treated with CX-4945; and 4) group 4: treated with CX-4945, gemcitabine, and cisplatin. Drugs were administered in the following manner: gemcitabine, 15 mg/kg diluted in 0.1 ml saline intraperitoneal injection (IP) biweekly for 3 weeks; cisplatin, 4 mg/kg diluted in 0.1 ml saline IP weekly for 3 weeks; CX-4945, 100 mg/kg diluted in 0.2 ml 25 mM NaH2PO4 buffer by oral gavage twice daily biweekly for 5 weeks. Doses were determined and modified based on previous experiments and pharmaceutical company recommendations. Tumor sizes and mouse weights were compared between the four groups. Animals were euthanized 35 days after administration of each drug; tumors were resected and subjected to Ki-67 and TUNEL assays. The treatment period was recommended by the drug company which developed the drug of interest to avoid mouse intolerance and side effects.

Immunohistochemistry and Terminal Deoxynucleotidyltransferase dUTP Nick-End Labeling (TUNEL) Assay on Mouse Xenograft Tumors

Xenografts from euthanized mice were fixed in 4% paraformaldehyde for 48 hours, embedded in paraffin, and sectioned into 5.0-μm slices. Tumor tissues from six mice randomly selected from each group were sectioned and stained with hematoxylin and eosin (H&E) or by immunohistochemical staining for Ki67. The TUNEL assay was performed to assess apoptosis.

Tissue sectioning and immunohistochemical staining were performed at the Pathology Research Core at Mayo Clinic using the Leica Bond RX stainer (Leica, Buffalo, IL). Formalin-fixed, paraffin-embedded tissues were sectioned at 5 μm. IHC staining was performed online; tissue slides were dewaxed using Bond Dewax (Leica). Slides for Ki-67 stain were retrieved for 20 minutes using Epitope Retrieval 2 (EDTA; Leica). The Ki-67 (Clone EP5; Epitomics, #AC-0009) antibody used to stain these samples is a rabbit monoclonal and was diluted in Background Reducing Diluent (Dako, Carpinteria, CA) to 1:400. Primary antibody incubation was for 15 minutes.

The fluorescent TUNEL assay on xenografts (*In situ* cell death detection kit; Roche Applied Science) was performed on paraffin-embedded liver tissue sections. Briefly, paraformaldehyde-fixed, paraffin-embedded xenograft sections were deparaffinized and hydrated. The TUNEL assay was then performed using the manufacturer's protocol, and tissue slices were mounted with ProLong Gold antifade reagent with DAPI (Invitrogen). Apoptotic cells were quantified by counting TUNEL-positive nuclei in 5 random microscopic fields (63×) using the LSM780 confocal microscope (Zeiss, Jena, Germany).

Short Tandem Repeat (STR) Genotyping of CCA Cell Lines

Seventeen STR loci plus the gender-determining locus, Amelogenin, were amplified using the commercially available GenePrint 10 system from Promega. The cell line sample was processed using the Applied Biosystems 3730XL Genetic Analyzer. Data were analyzed using GeneMapper ID-X software (Applied Biosystems–ThermoFisher Scientific, Waltham, MA). Appropriate positive and negative controls were run and confirmed for each sample submitted (GENEWIZ Quotation Number: AW1408181).

Statistics

Data are expressed as the mean ± standard error of the mean (SEM) from at least three independent experiments. All statistical tests were performed using GraphPad Prism 5.0. Differences between groups were compared using an unpaired two-tailed t test. The tumor growth curves were compared using a nonlinear comparison of curves. Survival curves were compared using the log-rank test. $P < .05$ was considered statistically significant.

Results

Effect of CX-4945 on CCA Cell Viability

Treatment of the HuCCT1 cell line with CX-4945 for 24, 48, and 72 hours showed time-dependent inhibition of cell viability. Treatment with CX-4945 for 72 hours significantly inhibited viability of HuCCT1, EGI-1, and Liv27 cells in a dose-dependent manner with IC_{50} of 7.3, 9.5, and 9.4 μM, respectively (Figure 1*A*).

Effect of CX-4945 on Apoptosis

To further characterize CX-4945–induced cytotoxicity, caspase 3/7 activity was measured after cells were treated by CX-4945 for 24, 48, and 72 hours. At 24 hours, CX-4945 does not increase caspase 3/7 activity in all three cell lines even at high doses (e.g., 20 μM). At 48 hours, only higher doses (≥10 μM for HuCCT1 and Liv27 and ≥7.5 μM for EGI-1) significantly enhanced apoptosis of HuCCT1, EGI-1, and Liv27 cells ($P < .05$). At 72 hours, however, lower doses significantly enhanced apoptosis of all three cell lines (≥2.5 μM for HuCCT1, ≥5 μM for EGI-1 and Liv27) ($P < .05$) (Figure 1*B*). These findings were confirmed using a DAPI staining assay and fluorescence microscopy to assess morphologic changes of apoptosis (data not shown).

Effect of CX-4945 on Colony Formation Ability of CCA Cells

Next, we assessed the effect of CX-4945 on colony formation. Treatment with CX-4945 for 10 days significantly reduced the colony-forming ability of HuCCT1 and EGI-1 cells in a dose-dependent manner

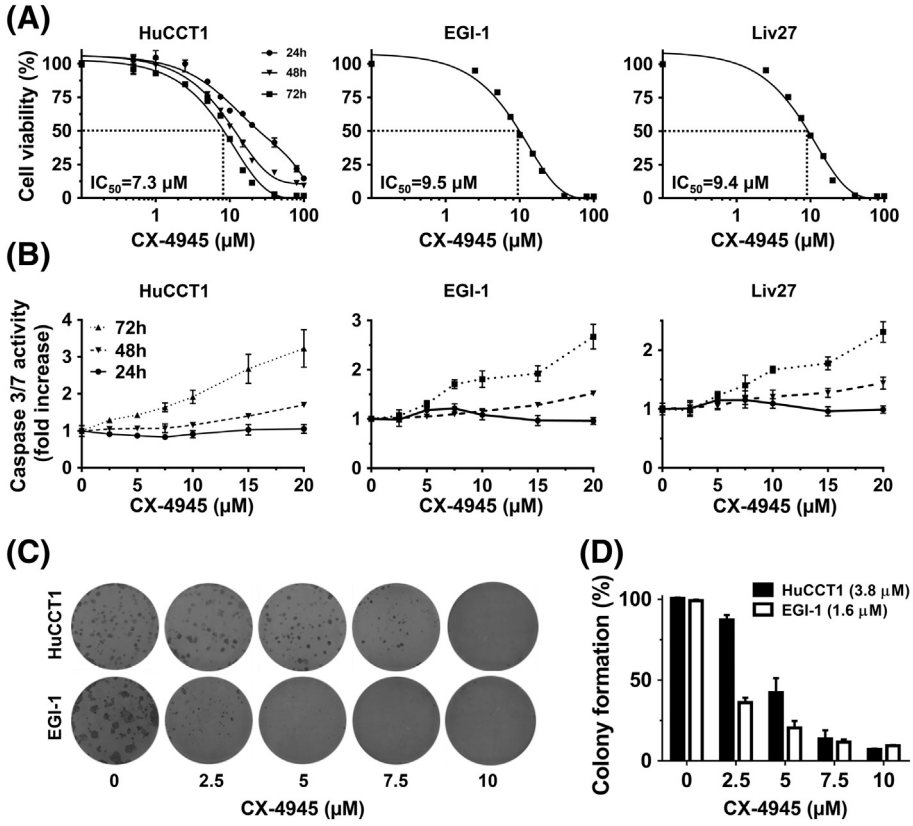

Figure 1. CX-4945 decreases cell viability of HuCCT1, EGI-1, and Liv27 CCA cell lines in dose-dependent manner (IC_{50} of 7.3, 9.5, and 9.4 μM, respectively) (A). CX-4945, only at higher doses and longer exposure, increases caspase 3/7 activity of all three cell lines (B). CX-4945 significantly decreased the colony-forming ability of HuCCT1 and EGI-1 cells (IC_{50} of 3.8 and 1.6 μM, respectively) (C).

with an IC_{50} of 3.8 and 1.6 μM, respectively (Figure 1, *C* and *D*). These results confirm that treatment with CX-4945 inhibits CCA cell colony formation in a dose-dependent manner.

CX-4945-induced inhibition of CK2

As expected, CX-4945 significantly inhibited CK2 phosphorylation in all three CCA cells in a dose-dependent manner. For example, at the 2.5-μM dose, CX-4945 decreased P-CK2/total-CK2 ratio by 27%, 23%, and 25% in HuCCT1, EGI-1, and Liv27 cells, respectively ($P < .05$). At higher doses (e.g., 10 μM), CX-4945 decreased the P-CK2/total-CK2 ratio by 96%, 99%, and 94% in HuCCT1, EGI-1, and Liv27 cells, respectively ($P < .05$) (Supplementary Figure 1, *A* and *B*). These findings confirm that CX-4945 inhibits CK2 in CCA cells.

Effect of CX-4945 on Cellular Signaling Pathways

Treatment of HuCCT1 cells with CX-4945 inhibited AKT phosphorylation at positions S129 and S473 in a dose-dependent manner with a P-AKT/total-AKT ratio reduction of 98% ($P = .004$) and 75% ($P = .0002$), respectively, at the 2.5-μM dose (Figure 2, *A* and *B*). Similarly, profound reductions of the P-AKT/total-AKT ratio were achieved by treatment of EGI-1 cells. Treatment of the Liv27 cell line, which was established from a CCA known to bear an activating mutation in the PIK3CA gene, resulted in a less profound reduction in the P-AKT/total-AKT ratio at the 2.5-μM dose, suggesting that the PIK3CA mutation may render this cell line partially resistant to the effects of PI3K/AKT pathway inhibition.

Treatment of HuCCT1 cells with CX-4945 inhibited the phospho-PTEN/Total PTEN ratio by 48% at the 2.5-μM dose ($P = .006$) (Figure 2, *A* and *C*). Similarly, PTEN phosphorylation was inhibited by similar percentages in EGI-1 cells (Figure 2, *A* and *C*). Interestingly, for Liv27 cells, the observed reduction in phospho-PTEN was accompanied by a corresponding reduction in total PTEN levels, suggesting that in certain contexts CX-4945 may also act through mechanisms that suppress total PTEN protein levels.

To determine whether downstream elements of the PI3K/AKT signaling pathway are modulated upon treatment with CX-4945, we assessed the effect of CX-4945 on mTOR and p70 S6K molecules. In HuCCT1 and Liv27 cells, only higher doses of CX-4945 (7.5 and 10 μM) inhibited the phospho-mTOR/Total mTOR ratio (33.7% and 72.3% for HuCCT1 and 10.2% and 26.6% for Liv27, respectively) ($P < .05$) (Supplementary Figure 1, *A* and *B*). In EGI-1 cells, on the other hand, the effect of CX-4945 on phospho-mTOR/Total mTOR ratio was paradoxical with ratio increased by 17% when cells were treated with 2.5 μM (Supplementary Figure 1, *A* and *B*). Similarly, only higher doses of CX-4945 (7.5 and 10 μM) inhibited phospho-p70 S6K/total p70 S6K ratio in HuCCT1 and Liv27 cells (by 22.1% and 36.4% in HuCCT1, 17% and 71.9% in Liv27, respectively) ($P < .05$). In EGI-1 cells, this ratio was increased with treatment with CX-4945 (ratio increased by almost nine-fold when cells treated with CX-4945 2.5 μM) (Supplementary Figure 1, *A* and *B*).

Overall, these findings suggest that inhibition of PI3K/AKT pathway by CX-4945 at least partially mediates the antineoplastic effect of CX-4945 in CCA cells.

Additive Effect of CX-4945 with Gemcitabine or Cisplatin

All three CCA cells were treated with a range of doses of CX-4945 and of gemcitabine or cisplatin (Supplementary Figures 2, 3, and 4). In HuCCT1 cells, treatment with gemcitabine 10 nM combined with 5

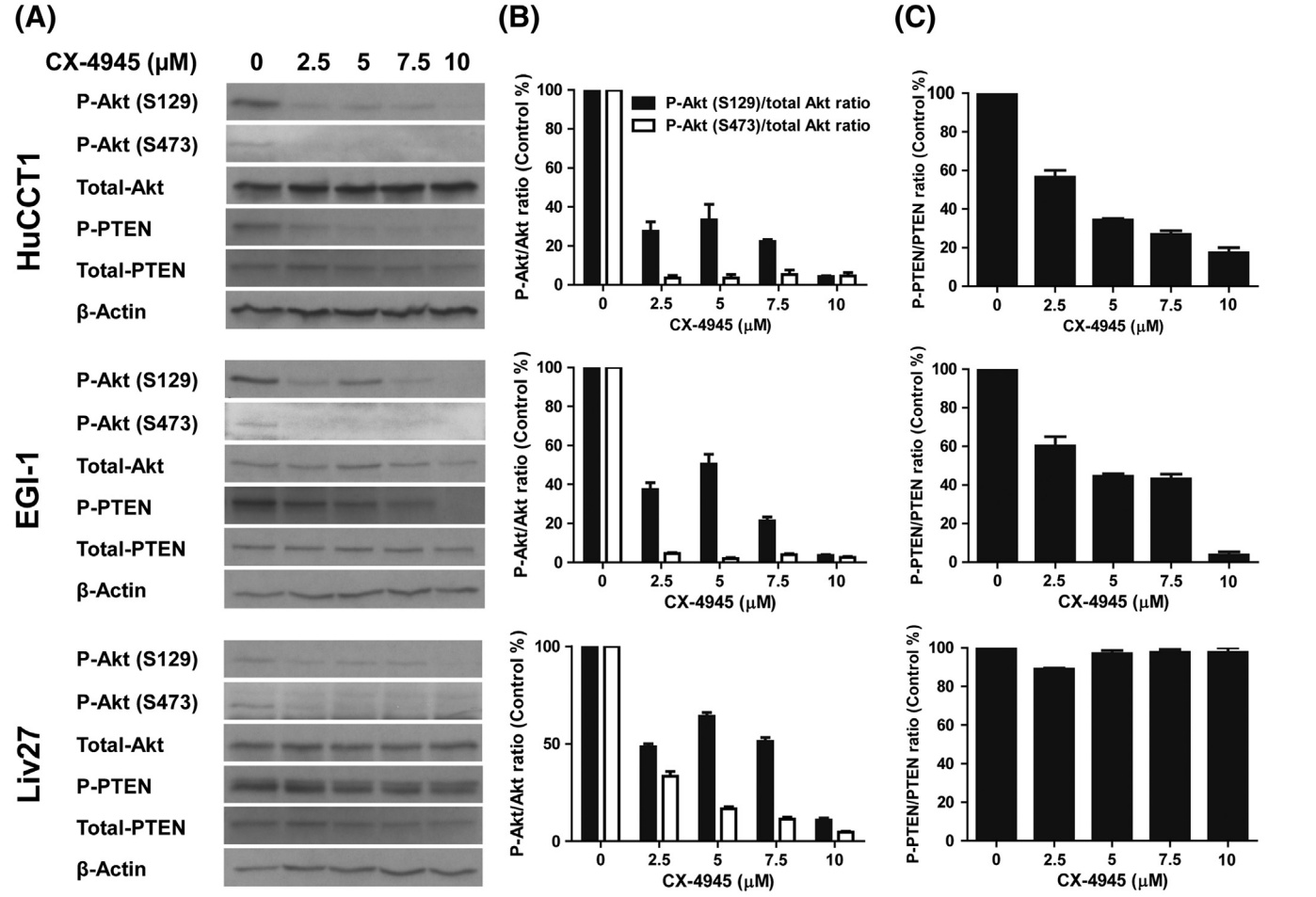

Figure 2. CX-4945 treatment of HuCCT1, EGI-1 and Liv27 decreases phosphorylation of Akt (A and B) and of PTEN (only in HuCCT1 and EGI-1 cells) (A and C).

or 7.5 μM CX-4945 reduced cell viability by an additional 15% ($P < .001$, CI = 0.86) or 25% ($P < .001$, CI = 0.86), respectively, compared to the effect of gemcitabine alone (Figure 3*A*). Treatment with 1 μM cisplatin combined with 5 or 7.5 μM CX-4945 also reduced cell viability of HuCCT1 by an additional 20% ($P < .001$, CI ≈ 1) or 35% ($P < .001$, CI ≈ 1), respectively, compared to the effect of cisplatin alone (Figure 3*A*).

Similarly, in EGI-1 cells, the combination of 10 nM gemcitabine with 5 or 7.5 μM CX-4945 decreased cell viability by an additional 30% ($P < .001$, CI = 0.9) or 40% ($P < .001$, CI ≈ 1), respectively, compared to gemcitabine alone (Figure 3*B*). Correspondingly, combination of 1 μM cisplatin with 5 or 7.5 μM CX-4945 decreased cell viability by an additional 25% ($P < .001$, CI ≈ 1) or 35% ($P < .001$, CI = 0.98), respectively, compared to cisplatin alone (Figure 3*B*).

However, consistent with the relative resistance of Liv27 to CX-4945, the effect of CX-4945 was less prominent in Liv27. Combination of 10 nM gemcitabine with 5 or 7.5 μM CX-4945 decreased cell viability by only 7% ($P < .05$, CI ≈ 1) or 16% ($P < .001$, CI ≈ 1), respectively, compared to gemcitabine alone (Figure 3*C*). Combination of 1 μM cisplatin with 5 or 7.5 μM CX-4945 decreased cell viability by 12% ($P < .05$, CI ≈ 1) or 15% ($P < .05$, CI ≈ 1), respectively, compared to cisplatin alone (Figure 3*C*).

Given that, for all cell lines and drug combinations, the CI falls between 0.8 and 1.2, these results show that CX-4945 has an additive (rather than synergistic) effect when combined with either gemcitabine or cisplatin in HuCCT1, EGI-1, and Liv27 cells with variable additional effects, particularly on the Liv27 cell line.

DNA-Effect of CX-4945 on DNA-Repairing Enzymes

Since gemcitabine and cisplatin both act by inducing DNA damage, we hypothesized that the additive effect of CK2 inhibition by CX-4945 with gemcitabine and cisplatin may be associated with inhibition of the DNA repair response (through XRCC1 and MDC1) to these agents.

In HuCCT1 cells, 10 μM CX-4945 significantly inhibited the phosphorylation of XRCC1 (at S485/T488 and S518/T519/T523) and MDC1 compared to control, decreasing P-XRCC1 (S485/T488)/XRCC1, P-XRCC1 (S518/T519/T523)/XRCC1, and P-MDC1/MDC1 ratios by 69% ($P = .02$), 71% ($P = .008$), and 59.6% ($P = .005$), respectively (Figure 4). In 10 nM gemcitabine–treated HuCCT1 cells, the ratios were 74%, 105%, and 93.2%, respectively. These ratios were significantly inhibited after adding 10 μM CX-4945 by 31.9% ($P = .007$), 43.8% ($P = .004$), and 11.3% ($P = .0008$), respectively. Treating HuCCT1 cells with 1 μM cisplatin increased P-XRCC1 (S485/T488)/XRCC1, P-XRCC1 (S518/T519/T523)/XRCC1, and P-MDC1/MDC1 ratios by 38.2% ($P = .01$), 30.9% ($P = .01$), 9.3% ($P = .01$), respectively, compared to control, consistent with activation of DNA repair pathways. Adding 10 μM CX-4945 to cisplatin decreased the ratios by 83.9%, 108.6%, and 67.4% compared to control,

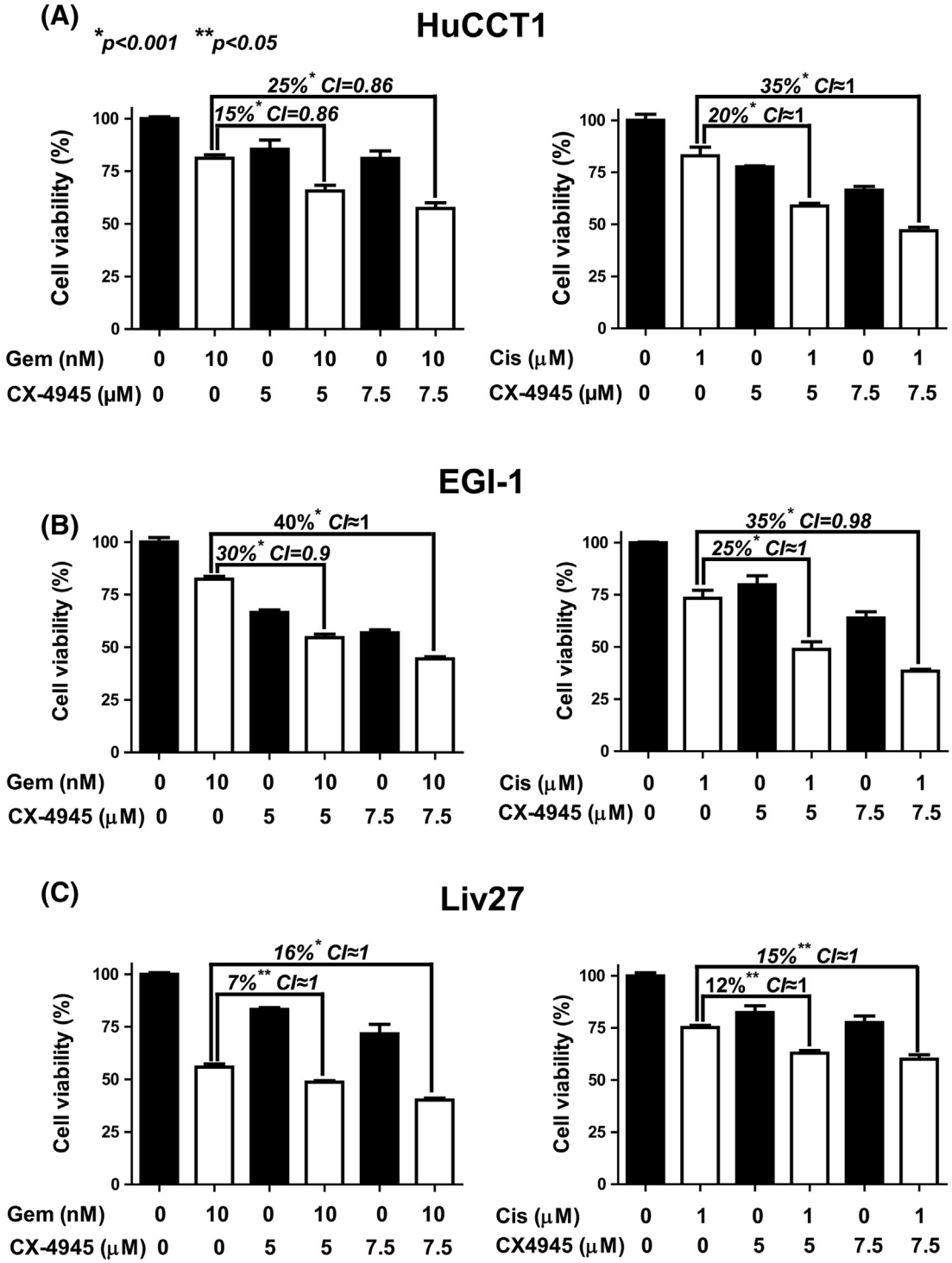

Figure 3. CX-4945 enhances the cytotoxic effect of gemcitabine (Gem) or cisplatin (Cis) in HuCCT1 (A), EGI-1 (B), and LIV27 (D) cells with IC_{50} range between 0.8 and 1.2, indicating an additive effect.

respectively, showing that CX-4945 is able to abrogate the DNA repair response induced by cisplatin (Figure 4).

In EGI-1 cells, 10 μM CX-4945 significantly inhibited the phosphorylation of both XRCC1 and MDC1 compared to control, decreasing the percentages of P-XRCC1 (S485/T488)/XRCC1, P-XRCC1 (S518/T519/T523)/XRCC1, and P-MDC1/MDC1 ratios by 47.1% (P = .01), 38.9% (P = .07), and 49.3% (P = .08), respectively (Figure 4). In a difference from the response of HuCCT1 cells to gemcitabine, treatment of EGI-1 cells with 10 nM gemcitabine induced XRCC1 and MDC1 phosphorylation compared to control, increasing the P-XRCC1 (S485/T488)/XRCC1, P-XRCC1 (S518/T519/T523)/XRCC1, and P-MDC1/MDC1 ratios by 82% (P = .001), 26.7% (P = .09), and 40.1% (P = .05), respectively, compared to control. This activation was blocked by 10 μM CX-4945, which decreased the same ratios by 55.8% (P = .03), 46.8% (P = .04), and 121.4% (P = .006), respectively (Figure 4). Similarly, treating EGI-1 cells with 1 μM cisplatin increased P-XRCC1 (S485/T488)/XRCC1, P-XRCC1 (S518/T519/T523)/XRCC1, and P-MDC1/MDC1 ratios by 53.1% (P =

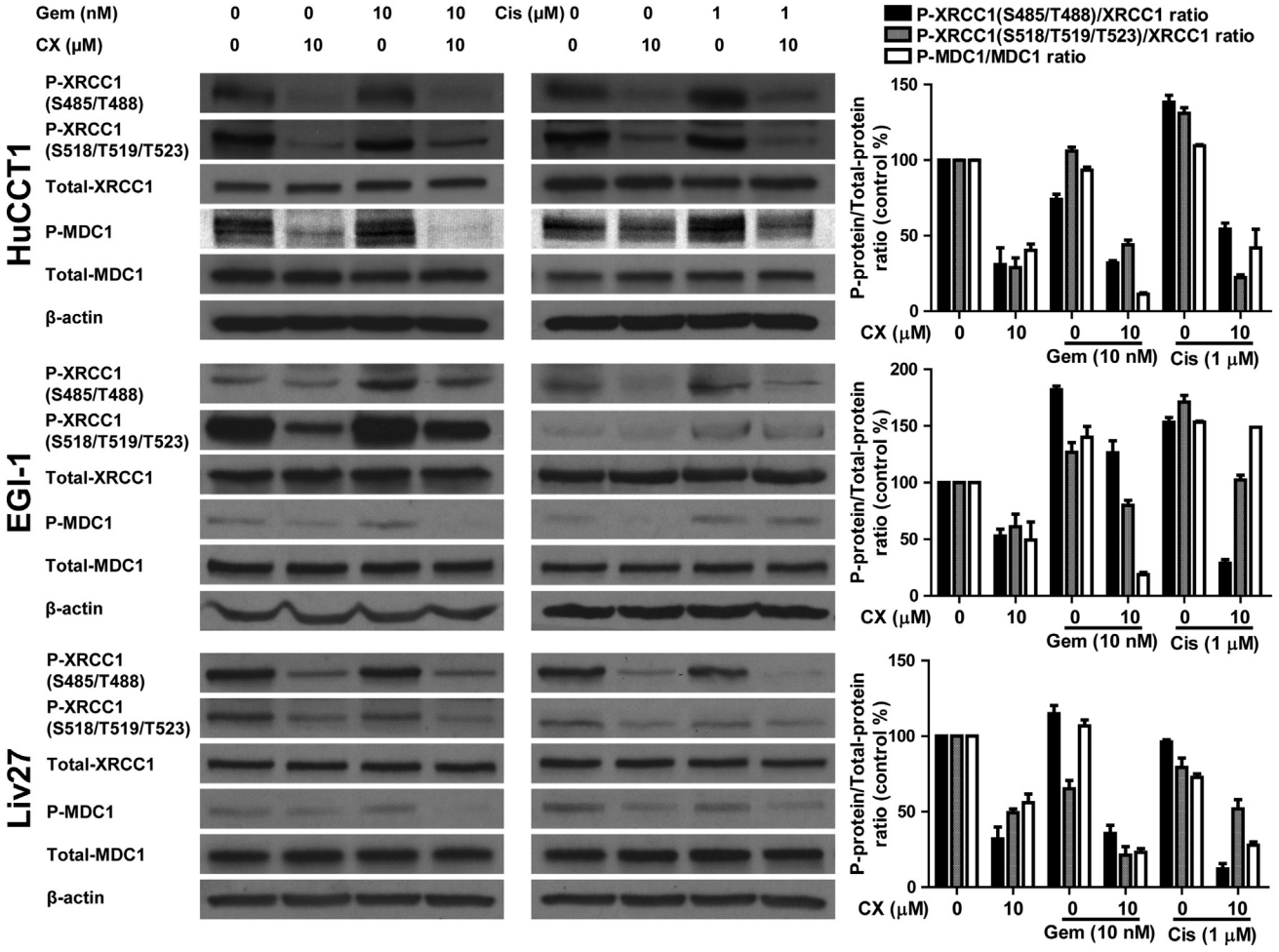

Figure 4. CX-4945 significantly inhibits the phosphorylation of the DNA-repairing enzymes XRCC1 and MDC1.

.006), 71% (P = .007), and 53.5% (P = .0003), respectively, compared to control. Adding 10 μM CX-4945 to cisplatin decreased the ratios by 124.4% (P = .001), 68.7% (P = .01), and 4.5% (P = .03), respectively (Figure 4). Interestingly, CX-4945 had clearly different relative effects on the P-XRCC1 (S485/T488)/XRCC1, P-XRCC1 (S518/T519/T523)/XRCC1, and P-MDC1/MDC1 ratios in the context of gemcitabine versus cisplatin treatment, with the largest inhibitory effect on the P-MDC1/MDC1 ratio in the context of gemcitabine treatment, while in the context of cisplatin treatment, the P-XRCC1 (S485/T488)/XRCC1 ratio was the most profoundly affected (Figure 4).

After treatment of Liv27 cells, neither gemcitabine nor cisplatin produced substantial increases in the P-XRCC1 (S485/T488)/XRCC1, P-XRCC1 (S518/T519/T523)/XRCC1, and P-MDC1/MDC1 ratios; otherwise, regarding the effect of CX-4945 on the DNA repair enzymes, we obtained similar results: 10 μM CX-4945 decreased P-XRCC1 (S485/T488)/XRCC1, P-XRCC1 (S518/T519/T523)/XRCC1, and P-MDC1/MDC1 ratios by 68% (P = .01), 50.7% (P = .002), and 43.9% (P = .01), respectively, compared to control (Figure 4). After gemcitabine treatment, P-XRCC1 (S485/T488)/XRCC1, P-XRCC1 (S518/T519/T523)/XRCC1, and P-MDC1/MDC1 ratios were 114.8% (P = .01), 65% (P < .001), and 106.7% (P = .07), respectively, compared to control. In the context of gemcitabine treatment, 10 μM CX-4945 inhibited gemcitabine-induced phosphorylation of XRCC1 (P = .003) compared to control. Similarly, cisplatin did not increase the phosphorylation of XRCC1 and MDC1 compared to control, producing ratios of 96% (P = .11), 79.3% (P = .08), and 72.7% (P = .007), respectively, compared to control. However, adding CX-4945 to cisplatin inhibited the phosphorylation of XRCC1 and MDC1 significantly by ratios of 84% (P = .002), 27.5% (P = .08), and 44.9% (P = .005), respectively (Figure 4).

To validate that CX-4945 enhances the effect of gemcitabine and cisplatin through inhibiting DNA repairing enzymes, we knocked down XRCC1 and MDC1 using shRNA and assessed caspase 3/7 activity in HuCCT1 and EGI-1 cells (Supplementary Figure 5). XRCC1 knockdown was associated with 0.36- and 0.63-fold increase in caspase 3/7 activity in HuCCT1 and EGI-1 cells, respectively (P < .05). MDC1 knockdown, on the other hand, was associated with decrease (0.3- and 0.2-fold in HuCCT1 and EGI-1, respectively) (P < .05) in caspase 3/7 activity (Supplementary Figure 5, *A* and *B*).

Overall, these finding suggest that CX-4945 inhibits the DNA repair response induced by gemcitabine or cisplatin through its known effect of inhibiting the activation of DNA-repairing enzymes (particularly XRCC1) but also demonstrate that there is substantial CCA cell variability in the DNA repair response to gemcitabine or cisplatin as well as in the responsiveness of the DNA repair enzyme apparatus to CX-4945.

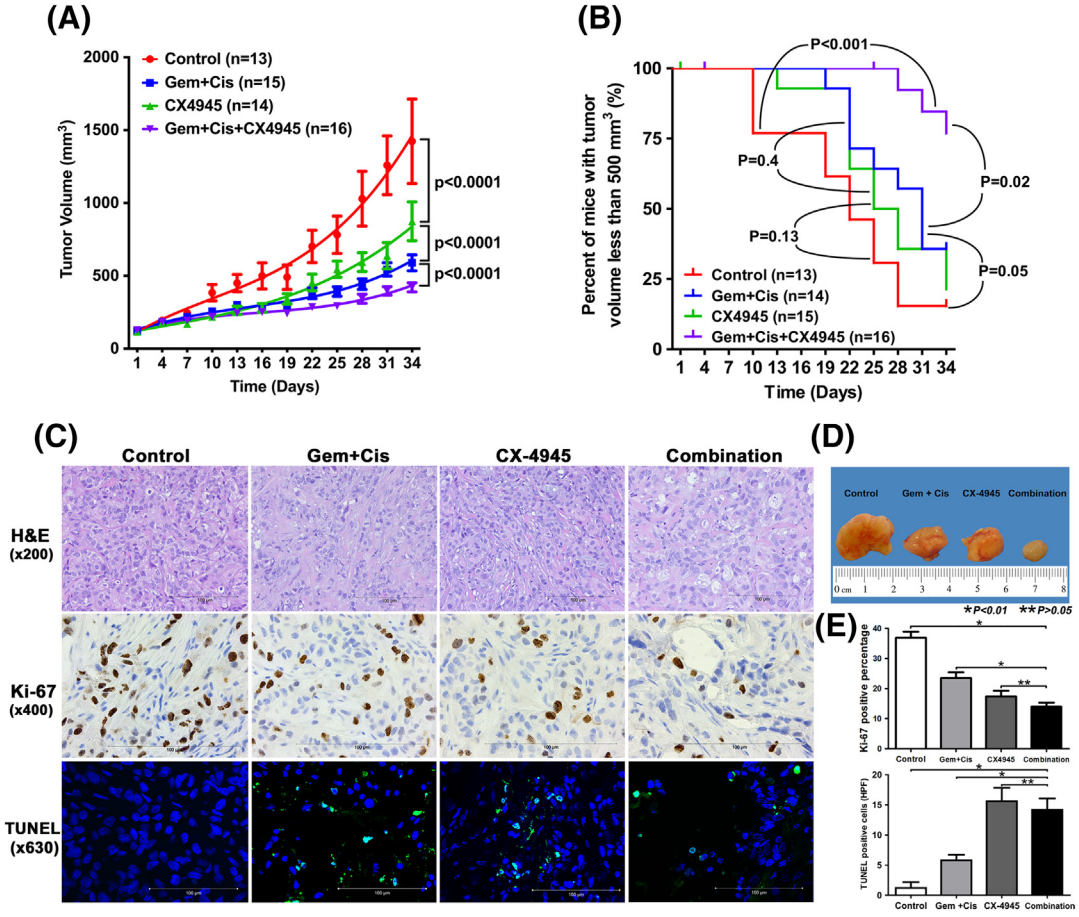

Figure 5. CX-4945 reduces tumor growth compared to control (A) and enhances the effect of the standard therapy, gemcitabine (Gem) and cisplatin (Cis), on tumor growth (A and D). CX-4945 also improves survival of mice when added to gemcitabine and cisplatin (B). CX-4945 significantly decreases CCA cell proliferation in xenografts compared to the control ($P < .0001$) and gemcitabine and cisplatin ($P = .02$) (C and E). CX-4945 in combination with gemcitabine and cisplatin decreases cell proliferation compared to gemcitabine and cisplatin ($P < .0001$) (C and E). CX-4945 increases apoptosis in xenografts compared to control and gemcitabine/cisplatin (C and E).

Effect of CX-4945 Alone on Growth of HuCCT1 Xenograft Tumors

To determine whether the additive effect of CX-4945 with gemcitabine or cisplatin *in vitro* could be translated into increased antitumor efficacy *in vivo*, we tested these combinations in a xenograft model. For this purpose, we selected the HuCCT1 model because it is aggressively tumorigenic and allows us to investigate Ki-67/TUNEL staining as pharmacodynamic biomarkers of combination activity in tumors. Also, as mentioned above, HuCCT1 is associated with high expression of CK2. At day 34 of treatment, tumors implanted in CX-4945–treated mice had significantly less tumor volume than control mice, with mean tumor volumes of 874.5 ± 499.4 mm^3 versus 1423.3 ± 1043.7 mm^3, respectively ($P < .0001$ for comparison of the curves) (Figure 5, *A* and *D*). Standard treatment with combination gemcitabine and cisplatin was significantly more potent than CX-4945 alone (P .0001) (Figure 5, *A* and *D*). Survival curves showed a trend towards improved survival (assessed by number of mice with tumor volume <500 mm^3) in mice treated with CX-4945 alone compared to controls ($P = .13$) (Figure 5*B*). The body weights of the mice treated with CX-4945 alone were not different from those of controls.

Effect of CX-4945 in Combination with the Standard Therapy on HuCCT1 Xenograft Model

As expected, gemcitabine and cisplatin significantly inhibited tumor growth ($P < .0001$) (Figure 5, *A* and *D*). Combining CX-4945 with gemcitabine and cisplatin (group 4) showed a more potent effect on tumor growth than gemcitabine and cisplatin (group 2) (with mean tumor volumes of 421.2 ± 112.8 mm^3 vs 657.1 ± 176.3 mm^3, respectively, $P < .0001$) (Figure 5, *A* and *D*). Survival curves showed significantly improved survival in group 4 compared to group 1 ($P < .001$) and group 2 ($P = .02$) (Figure 5*B*). At the end of the experiment (day 34), six out of seven (85%) mice alive in group 4 had tumor volumes less than 500 mm^3 versus three out of nine (33%) of the mice alive in group 2. These results indicate that CX-4945 exerts an anticancer effect on CCA *in vivo* and enhances the effect of standard therapy with gemcitabine and cisplatin. The body weights of mice in group 4 were not different from weights of mice in group 2. Cisplatin treatment is known to be associated with decreased body weight of treated animals. In the gemcitabine- and cisplatin-treated groups, body weights of the mice declined compared to controls, while the body weights of mice treated with CX-4945 alone did not show a significant decline. Body weights of mice treated with

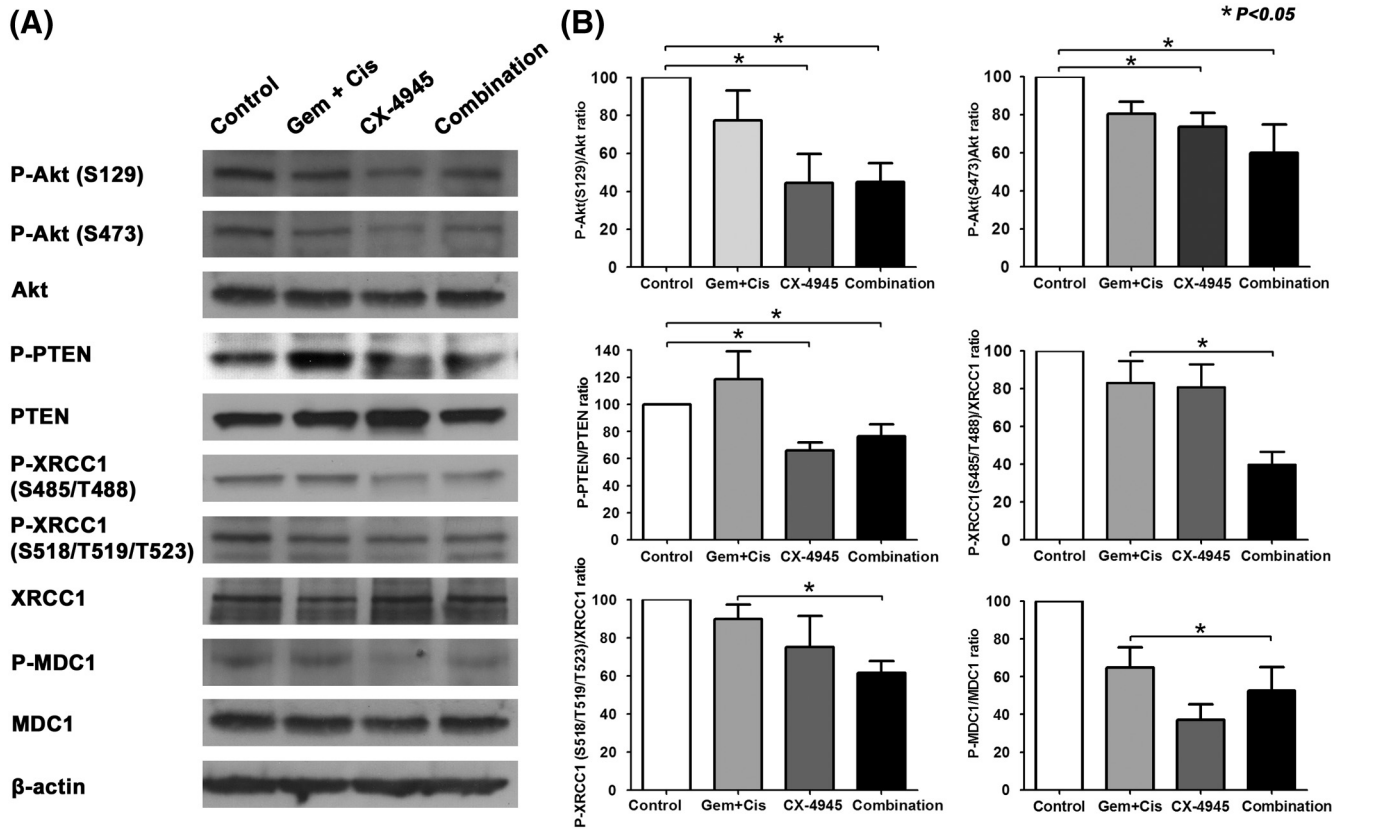

Figure 6. CX-4945 treatment in xenograft tissues was associated with inhibition of AKT pathway and DNA-repairing enzymes compared to control or standard therapy, gemcitabine (Gem) and cisplatin (Cis).

cisplatin recovered rapidly after suspension of cisplatin treatment (3 weeks after starting the treatments).

Validation of CX-4945 Effect on Cell Proliferation and Apoptosis in Xenograft Model

H&E staining of xenografts from each group showed similar moderately differentiated adenocarcinoma (Figure 5*C*). Tumor staining using the Ki-67 assay showed decreased CCA cell proliferation in xenografts from mice treated with CX-4945 alone compared to the control group ($P < .0001$) as well as mice treated with gemcitabine and cisplatin ($P = .02$) (Figure 5, *C* and *E*). In mice treated with CX-4945 in combination with gemcitabine and cisplatin, cell proliferation was significantly decreased compared to mice treated with gemcitabine and cisplatin ($P < .0001$). However, there was no statistically significant difference in inhibition of cell proliferation between mice treated with CX-4945 alone and those treated with CX-4945 in combination with gemcitabine and cisplatin ($P = .14$).

TUNEL staining assays showed significantly increased apoptosis in mice treated with CX-4945 compared to controls ($P = .0004$) and mice treated with gemcitabine and cisplatin ($P = .003$) (Figure 5, *C* and *E*). Apoptotic activity in tumors from mice treated with CX-4945 in combination with gemcitabine and cisplatin was significantly increased compared to controls ($P = .0003$) or mice treated with gemcitabine and cisplatin ($P = .003$); however, there was no significant difference compared to CX-4945–treated tumors ($P = .6$) (Figure 5, *C* and *E*).

Effect of CX-4945 on the PI3K/AKT Pathway and DNA-Repairing Enzymes In Vivo

We showed above that CX-4945 inhibited the PI3K/AKT pathway and the DNA repair enzymes XRCC1 and MDC1 in three different cell lines. These findings were confirmed in the HuCCT1 xenograft model. Treatment with CX-4945 alone significantly inhibited AKT (at S129 and S473) and PTEN phosphorylation compared to controls and tumors from mice treated with gemcitabine and cisplatin. CX-4945 reduced P-AKT (S129)/AKT and P-AKT (S473)/AKT ratios by 55% ($P = .004$) and 26% ($P = .003$), respectively, compared to control. Similarly, CX-4945 reduced the P-PTEN/PTEN ratio by 34% ($P = .0002$) compared to control. Gemcitabine and cisplatin did not significantly inhibit phosphorylation of AKT (S129) or PTEN compared to control. However, they did inhibit the phosphorylation of AKT at S473, reducing the P-AKT (S473)/AKT ratio by 20% ($P = .009$). The combination of CX-4945 with gemcitabine and cisplatin significantly decreased the phosphorylation of AKT (S129), AKT (S473), and P-PTEN compared to control by 55%, 40.1%, and 25.4% (*P* values of .002, .03, and .01, respectively). However, this decrease was not significantly larger than the decrease produced by CX-4945 alone (*P* values of .98, .42, and .87, respectively), suggesting that the effect is mainly mediated by CX-4945 rather than by gemcitabine and cisplatin (Figure 6, *A* and *B*).

Treatment with gemcitabine and cisplatin did not significantly alter the phosphorylation of XRCC1 (S485/T488), XRCC1 (S518/T519/T523), or MDC1 in HuCCT1 mouse xenografts compared to

control with P-XRCC1 (S485/T488)/XRCC1, P-XRCC1 (S518/T519/T523)/XRCC1, and P-MDC1/MDC1 ratios of 83% ± 26.2%, 90% ± 16.6%, and 85% ± 47.5% (*P* values of .22, .24, and .1, respectively). Also, treatment with CX-4945 alone did not significantly inhibit phosphorylation of XRCC1 (S485/T488) and XRCC1 (S518/T519/T523) compared to control [P-XRCC1 (S485/T488)/XRCC1 ratio = 80.5% ± 27% and P-XRCC1 (S518/T519/T523)/XRCC1 ratio = 75% ± 36.6%; *P* values of .18 and .2, respectively). However, CX-4945 did significantly inhibit phosphorylation of MDC1 compared to control (P-MDC1/MDC1 ratio = 44.6% ± 19.6%, *P* = .001). Treatment with CX-4945, gemcitabine, and cisplatin significantly inhibited the phosphorylation of XRCC1 (S485/T488) and XRCC1 (S518/T519/T523) compared to treatment with gemcitabine and cisplatin [P-XRCC1 (S485/T488)/XRCC1 ratio = 39.8% ± 14.8%, P-XRCC1 (S518/T519/T523)/XRCC1 ratio = 61.5% ± 14%; $P < .05$]; however, it did not significantly inhibit the phosphorylation of MDC1 compared to CX-4945 alone (P-MDC1/MDC1 ratio = 52.5% ± 28%, *P* = .1) (Figure 6, *A* and *B*).

STR Profile of CCA Cells (Supplementary Table 1)

The submitted sample Liv27 profile did not exactly match any cell line within the Deutsche Sammlung von Mikroorganismen und Zellkulturen GmbH (DSMZ) database. The profiles for EGI-1 matched the equivalent genotyping profile for EGI-1 in the DSMZ database (DSMZ No. 385). The profiles for HuCCT1 also matched the equivalent genotyping profile for HuCCT1 in the DSMZ database (DSMZ cell No. JCR30425 and RCB 1960).

Discussion

Elevated activity of CK2 has been associated with progression of different cancers [2,15]. High CK2 expression has been detected in 66% of CCA tissues and was associated with more aggressive disease and poorer overall survival [5]. CX-4945, a potent CK2 inhibitor, was previously studied as a therapeutic agent in different malignancies such as hematologic malignancies [16]; pancreatic adenocarcinoma [4]; ovarian cancer [8]; and lung [17], head and neck [11,18], and breast [19] cancers. CX-4945 exerts its effects mainly through blocking the action of CK2 on different components of the PI3K/AKT pathway, particularly inhibiting phosphorylation of the AKT and PTEN molecules [4]. The PI3K/AKT pathway plays an important role in the aggressiveness of cholangiocarcinoma [10], and it has been implicated in the pathogenesis of this cancer [20]. Other studies have shown that increased levels of phosphorylated AKT were present in >80% and >60% of extrahepatic [21] and intrahepatic [22,23] CCAs, respectively. In the present study, we confirmed that CX-4945, *via* inhibiting CK2, significantly inhibits the cell viability of HuCCT1, EGI-1, and Liv27 CCA cells (Figure 1*A*). CX-4945 also significantly inhibited the colony-forming ability of both HuCCT1 and EGI-1 cells (Figure 1, *C* and *D*). The effect of CX-4945 on colony-forming ability of Liv27 was not assessed due to the fact that these cells did not show any ability to form colonies. Although CX-4945 alone significantly inhibited tumor volumes in mice compared to control, there was no improvement in mice survival after 34 days of treatment (Figure 5, *A* and *B*). We found that CX-4945 inhibited the PI3K/AKT pathway through inhibition of AKT phosphorylation (at both S129 and S473), (and thus decreasing its effect) and PTEN phosphorylation (rendering PTEN active, blocking PIP3 formation and therefore inhibiting the AKT pathway) in three CCA cell lines (Figure 2, *A-C*) as well as in a CCA xenograft model (Figure 6). The net effect of dephosphorylating the AKT molecule is a decrease in CCA cell proliferation. The effect of CX-4945 on AKT downstream elements mTOR and p70 S6K was only noticed in HuCCT1 and Liv27 and only with higher doses (7.5 and 10 μM), confirming that other molecules can be modulated and contribute to the antineoplastic effect of CX-4945.

Even though previous studies have shown that CK2 inhibition induced apoptosis in various cancer cells [24–26], we found that CX-4945 increases caspase 3/7 activity in a dose- and time-dependent manner, with lower doses and shorter exposure time leading to no increase in apoptosis (Figure 1*B*). In mice experiment, we showed that CX-4945 significantly inhibited HuCCT1 cell proliferation and increased apoptotic activity compared to control. This suggests that, at low doses (and probably shorter time exposure), CX-4945 inhibits CCA cell viability primarily through inhibition of cell proliferation rather than by inducing apoptosis.

Our *in vivo* study confirmed that combining CX-4945 with both gemcitabine and cisplatin produced more antitumor efficacy against HuCCT1 xenografts than either the combination of gemcitabine and cisplatin or CX-4945 alone (Figure 5). At the doses given, CX-4945 alone was less effective than the combination of gemcitabine and cisplatin. Combination therapy with all three agents (gemcitabine + cisplatin + CX4945) significantly improved mouse survival compared to gemcitabine and cisplatin (*P* = .02). However, CX-4945 alone did not improve mouse survival compared to control.

Since CX-4945 blocks CK2 which is involved in many physiological pathways, we were concerned that it would cause severe adverse effects in the body; however, in our *in vivo* experiment, weight loss was primarily attributable to the combination of gemcitabine and cisplatin; after stopping gemcitabine and cisplatin (on day 21), mouse weights in those groups recovered rapidly and became comparable to mouse weights in groups not receiving gemcitabine and cisplatin. Therefore, the weight loss in group 4 was likely due to the adverse effect of gemcitabine and cisplatin, particularly cisplatin, which has been reported to induce significant weight loss [27]. These findings suggest that CX-4945 might be a safe and relatively nontoxic medication for use in humans.

Gemcitabine and cisplatin, the standard chemotherapy for CCA, are well-described DNA-damaging agents that have shown efficacy against a variety of cancers. The limited effect of gemcitabine and cisplatin against different cancers has been reported to be partially due to activation of DNA repair mechanisms in cancer cells [27–31]. Combining a DNA damaging-agent with a DNA repair inhibitor can theoretically present an effective approach in treating cancers. XRCC1 and MDC1 are key CK2-dependent mediators of the SSB and DSB repair machinery, respectively [8]. Blocking the effect of XRCC1 and MDC1 by CX-4945, a CK2 inhibitor, was confirmed as the mechanism of action behind the synergistic effect of CX-4945 with gemcitabine or cisplatin in ovarian cancer cells [8]. In this study, we showed that CX-4845 has an additive effect when combined with either gemcitabine or cisplatin in three different CCA cells. Our data suggest that CK2 might represent a rational therapeutic target that can be inhibited in combination therapy with other agents against CCA. Using Western immunoblotting, we showed that blocking CK2 with CX-4945 inhibited phosphorylation of both XRCC1 (at S485/T488 and S518/T519/T523 sites) and MDC1, blocking their ability to repair SSB and DSB induced by either gemcitabine or cisplatin. In mouse experiments, we confirmed that CX-4945 also blocks the effects of XRCC1 and MDC1 on DNA repair (Figure 6). Additionally, XRCC1 knockdown was associated with increased

caspase 3/7 activity in all three cell lines as compared to MDC1 knockdown which was associated with paradoxical small decrease in caspase activity (Supplementary Figure 5). These findings suggest that the additive effect of CX-4945 with the standard treatment might be explained by the inhibiting effect of CX-4945 on DNA repairing enzymes, particularly XRCC1.

In conclusion, we have demonstrated that targeting CK2 with CX-4945 has an antineoplastic effect and can enhance the effect of gemcitabine and/or cisplatin against CCA *in vitro* and *in vivo* through targeting the PI3K/AKT pathway and the DNA repair enzymes XRCC1 and MDC1. Given the demonstrated safety of CX-4945 in initial human studies, these preclinical data may justify clinical studies of CX-4945 or other CK2 inhibitors in CCA in combination with gemcitabine and cisplatin. A phase I/II randomized clinical trial is actively ongoing at different national and international institutions (including all three Mayo Clinic locations) to evaluate the effect of CX-4945 on patients with CCA with promising preliminary data.

Supplementary data to this article can be found online at https://doi.org/10.1016/j.tranon.2018.09.005.

Acknowledgement

This work was supported by National Institutes of Health grant CA165076 (to L. R. R.); the Mayo Clinic Center for Cell Signaling in Gastroenterology (NIDDK P30DK084567); The Cholangiocarcinoma Foundation; the Mayo Clinic Cancer Center (CA15083); and the Mayo Foundation. Its contents are solely the responsibility of the authors and do not necessarily represent the official views of the National Institutes of Health. We would also like to show our gratitude to the Senhwa Biosciences for sharing their CX-4945 with us during the course of this research.

References

[1] Njei B (2014). Changing pattern of epidemiology in intrahepatic cholangiocarcinoma. *Hepatology* **60**, 1107–1108.

[2] Ortega CE, Seidner Y, and Dominguez I (2014). Mining CK2 in cancer. *PLoS One* **9**e115609.

[3] Tawfic S, Yu S, Wang H, Faust R, Davis A, and Ahmed K (2001). Protein kinase CK2 signal in neoplasia. *Histol Histopathol* **16**, 573–582.

[4] Siddiqui-Jain A, Drygin D, Streiner N, Chua P, Pierre F, O'Brien SE, Bliesath J, Omori M, Huser N, and Ho C, et al (2010). CX-4945, an orally bioavailable selective inhibitor of protein kinase CK2, inhibits prosurvival and angiogenic signaling and exhibits antitumor efficacy. *Cancer Res* **70**, 10288–10298.

[5] Zhou F, Xu J, Ding G, and Cao L (2014). Overexpressions of CK2beta and XIAP are associated with poor prognosis of patients with cholangiocarcinoma. *Pathol Oncol Res* **20**, 73–79.

[6] Kotawong K, Thitapakorn V, Roytrakul S, Phaonakrop N, Viyanant V, and Na-Bangchang K (2016). Plasma peptidome as a source of biomarkers for diagnosis of cholangiocarcinoma. *Asian Pac J Cancer Prev* **17**, 1163–1168.

[7] Pierre F, Chua PC, O'Brien SE, Siddiqui-Jain A, Bourbon P, Haddach M, Michaux J, Nagasawa J, Schwaebe MK, and Stefan E, et al (2011). Discovery and SAR of 5-(3-chlorophenylamino)benzo[c][2,6]naphthyridine-8-carboxylic acid (CX-4945), the first clinical stage inhibitor of protein kinase CK2 for the treatment of cancer. *J Med Chem* **54**, 635–654.

[8] Siddiqui-Jain A, Bliesath J, Macalino D, Omori M, Huser N, Streiner N, Ho CB, Anderes K, Proffitt C, and O'Brien SE, et al (2012). CK2 inhibitor CX-4945 suppresses DNA repair response triggered by DNA-targeted anticancer drugs and augments efficacy: mechanistic rationale for drug combination therapy. *Mol Cancer Ther* **11**, 994–1005.

[9] Dokduang H, Juntana S, Techasen A, Namwat N, Yongvanit P, Khuntikeo N, Riggins GJ, and Loilome W (2013). Survey of activated kinase proteins reveals potential targets for cholangiocarcinoma treatment. *Tumour Biol* **34**, 3519–3528.

[10] Yothaisong S, Dokduang H, Techasen A, Namwat N, Yongvanit P, Bhudhisawasdi V, Puapairoj A, Riggins GJ, and Loilome W (2013). Increased activation of PI3K/AKT signaling pathway is associated with cholangiocarcinoma metastasis and PI3K/mTOR inhibition presents a possible therapeutic strategy. *Tumour Biol* **34**, 3637–3648.

[11] Zheng Y, McFarland BC, Drygin D, Yu H, Bellis SL, Kim H, Bredel M, and Benveniste EN (2013). Targeting protein kinase CK2 suppresses prosurvival signaling pathways and growth of glioblastoma. *Clin Cancer Res* **19**, 6484–6494.

[12] Buontempo F, Orsini E, Martins LR, Antunes I, Lonetti A, Chiarini F, Tabellini G, Evangelisti C, Melchionda F, and Pession A, et al (2014). Cytotoxic activity of the casein kinase 2 inhibitor CX-4945 against T-cell acute lymphoblastic leukemia: targeting the unfolded protein response signaling. *Leukemia* **28**, 543–553.

[13] Gomes AM, Soares MV, Ribeiro P, Caldas J, Povoa V, Martins LR, Melao A, Serra-Caetano A, de Sousa AB, and Lacerda JF, et al (2014). Adult B-cell acute lymphoblastic leukemia cells display decreased PTEN activity and constitutive hyperactivation of PI3K/Akt pathway despite high PTEN protein levels. *Haematologica* **99**, 1062–1068.

[14] Di Maira G, Gentilini A, Rovida E, Ottaviani D, Ruzzene M, and Marra F (2016). Role of the protein kinase CK2 in the biology of cholangiocarcinoma cells. *Dig Liver Dis* **48** (e20.

[15] Duncan JS and Litchfield DW (2008). Too much of a good thing: the role of protein kinase CK2 in tumorigenesis and prospects for therapeutic inhibition of CK2. *Biochim Biophys Acta* **1784**, 33–47.

[16] Chon HJ, Bae KJ, Lee Y, and Kim J (2015). The casein kinase 2 inhibitor, CX-4945, as an anti-cancer drug in treatment of human hematological malignancies. *Front Pharmacol* **6**, 70.

[17] Kim J and Hwan Kim S (2013). CK2 inhibitor CX-4945 blocks TGF-beta1–induced epithelial-to-mesenchymal transition in A549 human lung adenocarcinoma cells. *PLoS One* **8**e74342.

[18] Bian Y, Han J, Kannabiran V, Mohan S, Cheng H, Friedman J, Zhang L, VanWaes C, and Chen Z (2015). MEK inhibitor PD-0325901 overcomes resistance to CK2 inhibitor CX-4945 and exhibits anti-tumor activity in head and neck cancer. *Int J Biol Sci* **11**, 411–422.

[19] Gray GK, McFarland BC, Rowse AL, Gibson SA, and Benveniste EN (2014). Therapeutic CK2 inhibition attenuates diverse prosurvival signaling cascades and decreases cell viability in human breast cancer cells. *Oncotarget* **5**, 6484–6496.

[20] Ewald F, Grabinski N, Grottke A, Windhorst S, Norz D, Carstensen L, Staufer K, Hofmann BT, Diehl F, and David K, et al (2013). Combined targeting of AKT and mTOR using MK-2206 and RAD001 is synergistic in the treatment of cholangiocarcinoma. *Int J Cancer* **133**, 2065–2076.

[21] Chung JY, Hong SM, Choi BY, Cho H, Yu E, and Hewitt SM (2009). The expression of phospho-AKT, phospho-mTOR, and PTEN in extrahepatic cholangiocarcinoma. *Clin Cancer Res* **15**, 660–667.

[22] Schmitz KJ, Lang H, Wohlschlaeger J, Sotiropoulos GC, Reis H, Schmid KW, and Baba HA (2007). AKT and ERK1/2 signaling in intrahepatic cholangiocarcinoma. *World J Gastroenterol* **13**, 6470–6477.

[23] Javle MM, Yu J, Khoury T, Chadha KS, Iyer RV, Foster J, Kuvshinoff BW, Gibbs JF, Geradts J, and Black JD, et al (2006). Akt expression may predict favorable prognosis in cholangiocarcinoma. *J Gastroenterol Hepatol* **21**, 1744–1751.

[24] Faust RA, Tawfic S, Davis AT, Bubash LA, and Ahmed K (2000). Antisense oligonucleotides against protein kinase CK2-alpha inhibit growth of squamous cell carcinoma of the head and neck in vitro. *Head Neck* **22**, 341–346.

[25] Wang H, Davis A, Yu S, and Ahmed K (2001). Response of cancer cells to molecular interruption of the CK2 signal. *Mol Cell Biochem* **227**, 167–174.

[26] Slaton JW, Unger GM, Sloper DT, Davis AT, and Ahmed K (2004). Induction of apoptosis by antisense CK2 in human prostate cancer xenograft model. *Mol Cancer Res* **2**, 712–721.

[27] Siddik ZH (2003). Cisplatin: mode of cytotoxic action and molecular basis of resistance. *Oncogene* **22**, 7265–7279.

[28] Martin LP, Hamilton TC, and Schilder RJ (2008). Platinum resistance: the role of DNA repair pathways. *Clin Cancer Res* **14**, 1291–1295.

[29] Rosell R, Lord RV, Taron M, and Reguart N (2002). DNA repair and cisplatin resistance in non-small-cell lung cancer. *Lung Cancer* **38**, 217–227.

[30] Raoof M, Zhu C, Cisneros BT, Liu H, Corr SJ, Wilson LJ, and Curley SA (2014). Hyperthermia inhibits recombination repair of gemcitabine-stalled replication forks. *J Natl Cancer Inst* **106**.

[31] Helleday T, Petermann E, Lundin C, Hodgson B, and Sharma RA (2008). DNA repair pathways as targets for cancer therapy. *Nat Rev Cancer* **8**, 193–204.